

## Accepted Manuscript

Synthesis, structure, catalytic and magnetic properties of a pyrazole based five coordinated *di*-nuclear cobalt(II) complex

Rabiul Alam, Kaberi Pal, Bikash Kumar Shaw, Malay Dolai, Nabanita Pal, Shyamal Kumar Saha, Mahammad Ali

PII: S0277-5387(16)00003-6  
DOI: <http://dx.doi.org/10.1016/j.poly.2015.12.062>  
Reference: POLY 11761

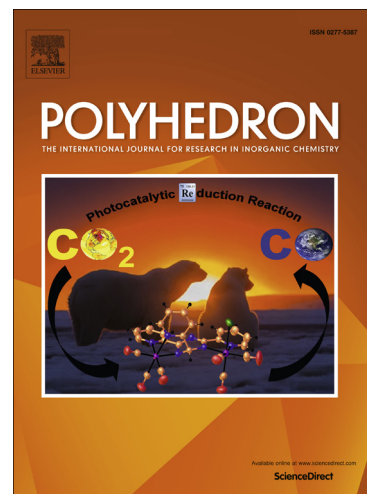
To appear in: *Polyhedron*

Received Date: 11 November 2015

Accepted Date: 20 December 2015

Please cite this article as: R. Alam, K. Pal, B.K. Shaw, M. Dolai, N. Pal, S.K. Saha, M. Ali, Synthesis, structure, catalytic and magnetic properties of a pyrazole based five coordinated *di*-nuclear cobalt(II) complex, *Polyhedron* (2016), doi: <http://dx.doi.org/10.1016/j.poly.2015.12.062>

This is a PDF file of an unedited manuscript that has been accepted for publication. As a service to our customers we are providing this early version of the manuscript. The manuscript will undergo copyediting, typesetting, and review of the resulting proof before it is published in its final form. Please note that during the production process errors may be discovered which could affect the content, and all legal disclaimers that apply to the journal pertain.



## Synthesis, structure, catalytic and magnetic properties of a pyrazole based five coordinated *di*-nuclear cobalt(II) complex

Rabiul Alam<sup>a</sup>, Kaberi Pal<sup>a</sup>, Bikash Kumar Shaw<sup>b</sup>, Malay Dolai<sup>a</sup>, Nabanita Pal<sup>a</sup>, Shyamal Kumar Saha<sup>b</sup> and Mohammad Ali<sup>a\*</sup>

<sup>a</sup> Department of Chemistry, Jadavpur University, Kolkata 700 032, India.

E-mail: [mali@chemistry.jdvu.ac.in](mailto:mali@chemistry.jdvu.ac.in)

<sup>b</sup> Department of Materials Science, Indian Association for the Cultivation of Science, Jadavpur, Kolkata 700032, India.

### Abstract

The reaction of 4-methyl-2,6-bis(3,5-dimethyl-1H-pyrazol-1-yl)methylphenol and  $\text{Co}(\text{NO}_3)_2 \cdot 6\text{H}_2\text{O}$  in MeCN gives rise to  $[\text{Co}_2(\text{L})_2(\text{N}_3)_2]$  (**1**), a dinuclear five coordinated complex of Co(II), in satisfactory yield. The complex has been characterized by C, H and N microanalyses, FT-IR and UV-Vis spectral measurements. A single crystal X-ray diffraction study of **1** reveals that each Co(II) atom is in a distorted square-pyramidal geometry. Electrochemical studies in  $\text{CH}_3\text{CN}$  showed that the Co(II)-Co(III)/Co(III)-Co(III) redox couple appears to be quasi-reversible ( $E_{1/2} = 0.409$  V), while the corresponding Co(II)-Co(III)/Co(II)-Co(II) couple is mostly irreversible ( $E_{1/2} = -0.447$  V). This complex displays modest catalytic activity towards the oxidation of various allylic compounds using TBHP as an oxidant in MeCN under mild conditions. A radical trapped experiment carried out in the presence of 4-*tert*-butylphenol clearly reveals that the epoxidation reactions occur purely through a radical pathway rather than a concerted one. Low temperature magnetic studies showed that the present Co(II) dimeric complex possesses a high positive magnetic anisotropy ( $D = + 29.8 \text{ cm}^{-1}$ ) and a weak ferromagnetic exchange interaction ( $2J = + 10.3 \text{ cm}^{-1}$ ).

**Keywords:** *di*-nuclear cobalt(II) complex; synthesis; structure; catalytic studies; magnetic properties.

## Introduction

Unique physical properties that correlate to novel modes of chemical reactivity are often displayed when a metal ion is in an unusual coordination geometry. In metalloenzymes such subtle structure/function relationships are exploited by intimately tuning the local stereochemistry and ligand-field of a protein active site to achieve specific catalytic transformations [1]. An appreciation of such specific ligand-to-metal interactions in protein active sites is therefore highly dependent on our basic understanding of the elementary stereochemical and ligand-field relationships in coordination chemistry [2-5]. These elementary principles are often employed to rationally design catalysts selective for specific transformations [6,7].

Since the discovery that the active site structure of methionine aminopeptidase (MAP, EC 3.4.11.18) contain a bis(*m*-carboxylato)dicobalt(II) core [8], the chemistry of dinuclear cobalt complexes has attracted major attention from coordination chemists to elucidate the relationship between dinuclear structures and their properties and functions.

Additionally, complexes with a high spin  $d^7$  configuration are of great interest owing to their interesting magnetic properties. The general approach is to use multidentate and bulky ligands that favor metal aggregation, keeping the resulting clusters well isolated from their neighbours [9]. Our interest lies in exploring the intrinsic properties that influence the electronic configuration of dinuclear high spin Co(II) complexes. Towards this end, a number of reports on dinuclear high-spin Co(II) complexes, viz.  $[\text{Co}_2(\text{tmpc})\text{Cl}_2][\text{CoCl}_4]$ ,  $[\text{Co}_2(\text{tmpc})\text{Cl}_2][\text{PF}_6]_2$ ,  $[\text{Co}_2(\text{tmpc})(\text{NO}_3)_2][\text{NO}_3]_2 \cdot \text{MeOH}$ ,  $[\text{Co}_2(\text{baib})(\text{Me-CO}_2)_3]\text{BPh}_4$  and  $[\text{Co}_2(\text{baib})(\text{PhCO}_2)_3]\text{BPh}_4$ , are available in the literature [10]. We are especially interested in the magnetism of dinuclear high spin cobalt(II) complexes since di- or polynuclear complexes with high magnetic spin and anisotropy may exhibit single-molecule magnetic (SMMs) behavior [11-14].

The cobalt(II) ion and its coordination complexes are well-known catalysts for the selective oxidation of alkanes and alkylbenzenes with molecular oxygen [15]. Cobalt(II/III) Schiff base complexes have also been found to be efficient catalysts for the epoxidation of olefins by molecular oxygen [16-20]. As an example, cobalt(II)-salen complexes were reported to show catalytic activity for the epoxidation of alkenes with  $\text{O}_2$  in the presence of a sacrificial co-reductant like isobutyraldehyde, 2-ethylbutyraldehyde etc [19-23]. Recently, the aerobic oxidation of alkenes over Co(II)-compounds with and without a co-reductant in DMF have also been

studied [24-26]. Here, DMF was regarded as a “sacrificial” solvent that functions as a co-reductant in the epoxidation reaction. Although there are number of reports where mononuclear cobalt complexes are used as catalysts in many organic transformation reactions [16-26], the use of the corresponding di- or polynuclear complexes for such purposes are rare. Herein, we report the synthesis, characterization through a single crystal X-ray diffraction study and magnetic susceptibility measurements, along with the catalytic activities towards the oxidation of olefins, namely cyclohexene, cyclooctene and styrene, in the presence of *tert*-butyl hydroperoxide (TBHP) of a homodinuclear complex ( $\text{LCo}^{\text{II}}_2$ ).

## Experimental section

### Materials and reagents.

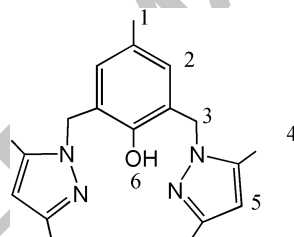
All chemicals were of analytical reagent grade and were used without further purification. Cobalt nitrate was purchased from Sigma-Aldrich.

### Physical measurements

Elemental analyses were carried out using a Perkin-Elmer 240 elemental analyzer.  $^1\text{H}$  NMR spectra were recorded in  $\text{CDCl}_3$  on a Bruker 300 MHz NMR spectrophotometer using tetramethylsilane ( $\delta = 0$ ) as an internal standard. Electronic spectra were recorded on an Agilent-8453 diode array UV-Vis spectrophotometer. The melting point was determined by an electro-thermal digital melting point apparatus (SUMSIM India) and is uncorrected. FTIR spectra (KBr disc) [(vs) = very strong, (s) = strong, (m) = medium and (w) = weak] were recorded with a Nicolet Magna-IR spectrophotometer (Series II). Mass spectra were recorded on an XEVO G2QTof spectrometer (Waters) with an electron spray ionization source. Electrochemical measurements were carried out using a computer controlled AUTOLAB (Model: AUTOLAB 302) cyclic voltammeter with a platinum (Pt) working electrode, a platinum-wire auxiliary electrode and an Ag/AgCl reference electrode. The supporting electrolyte is  $n\text{-Bu}_4\text{NClO}_4$  (0.1 M).

### Synthesis of 4-methyl-2,6-bis(3,5-dimethyl-1H-pyrazol-1-yl)methyl-phenol (HL):

4-Methyl-2,6-bis(3,5-dimethyl-1H-pyrazol-1-yl)methyl phenol was prepared using a reported method [27]. In a typical procedure 4-methyl-2,6-di(chloromethyl)phenol (1.68 g, 8.2 mmol) was dissolved in 15 ml dry THF in a round bottom flask. 1.57 g (16.4 mmol) 3,5-dimethyl pyrazole and 1.659 g (16.4 mmol) triethylamine ( $\text{Et}_3\text{N}$ ) were dissolved in 5-10 ml dry THF separately. The later solution was then added dropwise to the previous one with constant stirring. An instant precipitation of  $\text{Et}_3\text{NHCl}$  was observed and the colour of the solution turned bright yellow. After 24 hours of stirring the precipitate was filtered off. From the filtrate THF was removed under reduced pressure. Silicagel column chromatography was performed using DCM (dichloromethane) and methanol (7:3, v/v) as the eluent. The removal of solvent under reduced pressure afforded a light yellow solid in the pure form in 60% yield.  $^1\text{H}$  NMR ( $\text{CDCl}_3$ , 300 MHz)  $\delta$  (ppm): 2.07-2.20 (12H, s,  $-\text{CH}_3$ ), 2.48 (3H, s, Ar- $\text{CH}_3$ ), 5.08 (4H, s,  $-\text{CH}_2$ ), 5.83 (s, 2H,  $-\text{CH}$ ), 6.60 (2H, s,  $-\text{ArH}$ ), 10.36 (1H, brs,  $-\text{ArOH}$ ), (Fig. S1) IR ( $\text{cm}^{-1}$ ): 1640 ( $\text{C}=\text{N}$ ), 3400 ( $-\text{OH}$ ). (Fig.S2)



### Synthesis of complex (1)

**[ $\text{Co}_2(\text{L})_2(\text{N}_3)_2$ ]:** 4-Methyl-2,6-bis(3,5-dimethyl-1H-pyrazol-1-yl)methyl phenol (0.324 g, 1 mmol) was dissolved in MeCN, to which triethylamine (0.101 g, 1 mmol) was added dropwise with constant stirring.  $\text{Co}(\text{NO}_3)_2 \cdot 6\text{H}_2\text{O}$  (0.528 g, 2mmol) in 30 ml MeCN was then added dropwise to the above solution. After stirring for 30 min,  $\text{NaN}_3$  (0.13 g, 2 mmol) was added, stirring was continued for another 3 h and finally the resulting solution was filtered off and the filtrate was kept in a 100 ml beaker undisturbed. Slow evaporation afforded rod-shaped violet coloured crystals, suitable for X-ray studies, within 3 days. *Anal. Cal.* for  $\text{C}_{38}\text{H}_{46}\text{Co}_2\text{N}_{14}\text{O}_2$  (MW = 848.75): C, 53.78; H, 5.46; N, 23.10; *Found*: C, 52.78; H, 5.49; N, 23.11. IR ( $\text{cm}^{-1}$ ) 1642 ( $\text{C}=\text{N}$ ), 2045 ( $-\text{N}_3$ ) (Fig. S3).

**Table 1.**

### X-ray crystallography

Single crystal X-ray data of complex **1** were collected on a Bruker SMART APEX-II CCD diffractometer using graphite monochromated Mo-K $\alpha$  radiation ( $\lambda = 0.71073 \text{ \AA}$ ). Data collection, reduction, structure solution and refinement were performed using the Bruker APEX-II suite program (v 2.0-2). All available reflections to  $2\theta_{\text{max}}$  were harvested and corrected for Lorentz and polarization factors with Bruker SAINT plus. Reflections were then corrected for absorption, inter frame scaling and other systematic errors with SADABS [28]. The structure was solved by direct methods and refined by means of the full matrix least-square technique based on  $F^2$  with the SHELX-97 software package [29]. All the non-hydrogen atoms were refined with anisotropic thermal parameters. All the hydrogen atoms belonging to carbon and nitrogen atoms were placed in their geometrically idealized positions. Drawings of the molecules were generated with the program PLATON v-1.16. The crystallographic data for **1** are given in Table 1.

### Magnetic susceptibility measurements.

The temperature dependent magnetization was acquired with an MPMS XL-5 Quantum Design SQUID magnetometer on a polycrystalline sample in the range  $T = 2$  to 300 K, at  $B = 0.01 \text{ T}$ , and the isothermal magnetization was measured at  $T = 2.0, 4.0, 7.0$  and  $10 \text{ K}$  up to a magnetic field  $B = 5 \text{ T}$ . The experimental data were corrected for the diamagnetism of the constituent atoms using Pascal's constants and for the diamagnetism of the sample holder.

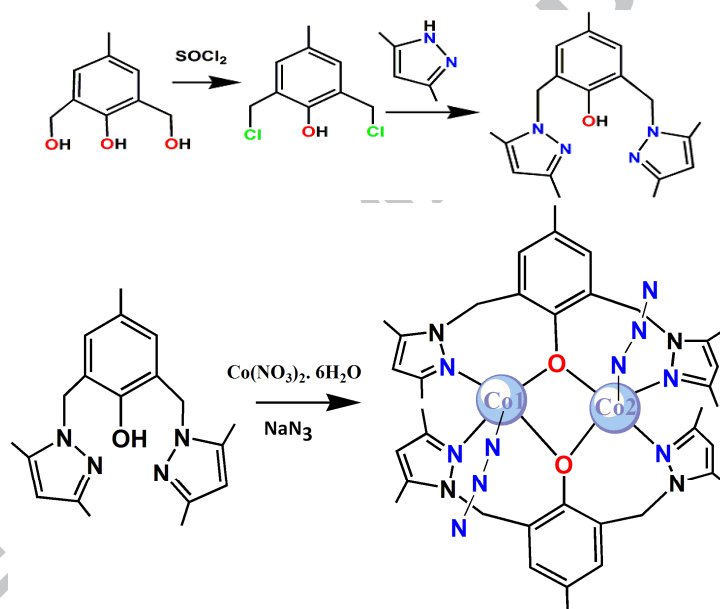
### Catalytic study

Allylic oxidation of various olefins was carried out using this material as a catalyst and *tert*-butylhydroperoxide (TBHP) as an oxidant. The overall reaction was performed in a two-necked round-bottomed flask fitted with a condenser and a temperature-controlled oil bath on a magnetic stirrer. In a typical procedure, 0.25 g of the substrate and TBHP oxidant (6 M in decane, Sigma-Aldrich) were taken (2:1 molar ratio) in 2.0 ml MeCN containing required amount (0.05 g, 0.059 mmol) of the catalyst. The temperature of the reaction was maintained at 50-55 °C and the products were collected at regular intervals. The progress of the reaction was monitored by an Agilent 7890D gas chromatograph (FID detector) fitted with a capillary column. The products were identified by a comparison with known standards.

## Results and Discussion

### Synthesis and structural description

2,6-Bis-(chloromethyl)-4-methyl-phenol was synthesized in a simple way by chlorination of the alcoholic group of 2,6-bis(hydroxymethyl)-4-methyl-phenol without protecting the phenolic OH group, as reported earlier, in a modest yield. This, on subsequent treatment with 3,5-dimethyl pyrazole in dry THF in presence of triethylamine (TEA) as a base, yields the novel ligand 2,6-bis-(3,5-dimethyl-pyrazol-1-ylmethyl)-4-methylphenol (HL) in ~90% yield. When it was treated with  $\text{Co}(\text{NO}_3)_2 \cdot 6\text{H}_2\text{O}$  in MeCN in presence of TEA and 2 equivalents of sodium azide, rod-shaped violet crystals suitable for X-ray diffraction were obtained on slow evaporation within 2-3 days.



Scheme 1

The results of single crystal X-ray diffraction analysis indicate that complex **1**, with a neutral dinuclear  $[\text{Co}^{\text{II}}_2(\text{L})_2(\text{N}_3)_2]$  core, crystallizes in the monoclinic system with the space group  $\text{C2/c}$ . The coordination environment around the  $\text{Co}^{\text{II}}$  ion is shown in Fig. 1, where the two cobalt atoms are centrosymmetric and coordinated by two tridentate ( $\text{N}_2\text{O}$ )  $\text{L}^-$  ligands and two azide ions, each having a distorted square pyramidal geometry. Co1 is coordinated by two N atoms (N1 and N3) from two 3,5-dimethyl pyrazole units belonging to two different ligands, one azide ion (N5) and one phenoxo O-atom (O1), which is further coordinated to second Co1a atom in a  $\mu_2$ -O fashion.

**Fig. 1.**

The Co1-N<sub>x</sub> distances (Table 2) ( $x = 1, 3$  and  $5$ ) are in the range 2.016-2.156 Å, while Co1-O1/O1a = 1.98 and 2.19 Å, which clearly indicate that the two Co1 atoms are in a highly distorted square pyramidal geometry. The geometry of a pentacoordinated metal centre can be measured by the Addison parameter ( $\tau$ ), which is calculated to be 0.88 ( $\tau = [(\alpha - \beta)/60] \times 100$ , where  $\alpha$  and  $\beta$  are the two largest ligand-metal-ligand angles of the coordination sphere) suggesting a distorted trigonal-bipyramidal geometry ( $\tau = 0$  for a perfect square pyramid and  $\tau = 1$  for a perfect trigonal bipyramid). This distortion may arise to avoid steric hindrance caused by the two methyl groups on two co-facially disposed 3,5-dimethyl pyrazole groups. The inter-metallic Co1...Co2 distance is found to be 3.198 Å. There are a number of intermolecular bifurcated H-bonding interactions between the N atom of the coordinated azide ion of one dinuclear unit and a methylenic-H atom of the pyrazole group and CH proton of the benzene ring belonging to a neighboring dinuclear complex, as portrayed in Fig. 2 and Table 3. The intramolecular  $\pi \cdots \pi$  interaction between two co-facial pyrazole rings strengthen the stability of the complex. All these interactions lead to a 1D supramolecular structure. The H-bonded close packing diagram of complex **1** is shown in Fig. 3.

**Fig. 2****Table 2****Fig. 3.**

### Bond Valence Sum (BVS) calculations.

Bond Valence Sum (BVS) [30] is a method very frequently used to examine the nature of the coordination and oxidation state of a central metal atom using crystallographic data for coordination complexes as well as for many biological molecules. The most successfully used empirical equation is:

$$\Sigma s_{ij} = \Sigma \exp[(R_o - R_{ij})/0.37]$$

where  $R_o$  is a parameter characteristic of the bond and  $R_{ij}$  are the crystallographically obtained



bond distances.  $\Sigma s_{ij}$  represents the charge on the central metal atom. From the calculations (Table S1) it can be seen that the oxidation state of the cobalt is 2.13 (Co1) and 2.12 (Co1a), which unequivocally indicate the +2 oxidation state for the Co atoms in complex **1**.

### UV-vis spectrum.

The UV spectrum of complex **1** in MeCN showed bands at 663 ( $\epsilon = 224 \text{ dm}^3 \text{ mol}^{-1} \text{ cm}^{-1}$ ) and 583 nm ( $\epsilon = 280 \text{ dm}^3 \text{ mol}^{-1} \text{ cm}^{-1}$ ), with a non-well resolved shoulder at 515 nm ( $\epsilon = 230 \text{ dm}^3 \text{ mol}^{-1} \text{ cm}^{-1}$ ) (Fig. 4), which may be assigned to  $^4T_{1g} \rightarrow ^4T_{2g}$  (F),  $^4T_{1g} \rightarrow ^4A_{2g}$  (F) and  $^4T_{1g} \rightarrow ^4T_{1g}$  (P) transitions, respectively. A comparison with other high spin, five-coordinated Co(II) spectra reveals a similarity to the known trigonal bipyramidal complexes, as expected on the basis of the crystal structure and magnetic moment [31-37].

Fig. 4

Fig. 5.

### Electrochemical studies

Complex **1** remains as a dinuclear entity, as evidenced from its HRMS spectrum. Complex **1** is electroactive in MeCN solution vs. Ag/AgCl. The two anodic peaks at -0.282 and 0.548 V correspond to the Co(II)-Co(II)  $\rightarrow$  Co(II)-Co(III) and Co(II)-Co(III)  $\rightarrow$  Co(III)-Co(III) oxidations, while the cathodic peaks at 0.270 and -0.611 V correspond to Co(III)-Co(III)  $\rightarrow$  Co(II)-Co(III) ( $E_{1/2} = 0.409 \text{ V}$ ) and Co(II)-Co(III)  $\rightarrow$  Co(II)-Co(II) ( $E_{1/2} = -0.447 \text{ V}$ ) reductions. While the Co(II)-Co(III)/Co(III)-Co(III) redox couple appears to be quasi-reversible, the corresponding Co(II)-Co(III)/Co(II)-Co(II) couple is mostly irreversible (Fig. 5).

### Magnetic study

To gain an insight into the magnetic property of this dimeric Co(II) complex, variable-temperature *dc* magnetic susceptibility measurements were performed between 2 and 300 K for a crystalline sample at a magnetic field of 100 Oe (Fig. 6). The thermal variation of the  $\chi_{MT}$  product is plotted after correcting for the diamagnetic contribution, as given in standard literature. This shows a room temperature value of around  $8.158 \text{ cm}^3 \text{ K mol}^{-1}$ , which is relatively

higher than the result for two uncoupled Co(II) ion spins (Fig. 7) [39]. The decrease in  $\chi_{\text{MT}}$  behavior down to 55 K is due to a temperature independent paramagnetic effect. Fitting of  $\chi_{\text{MT}}$  data, considering the temperature independent paramagnetic contribution (TIP), provides a small amount of TIP species ( $10^{-4} \text{ cm}^3 \text{ mol}^{-1}$ ). The extracted  $g$  parameter (Lande factor) is 2.39, which is also reasonable compared to the expected value obtained for an  $S = 3/2$  Co(II) system. As the temperature decreases, the  $\chi_{\text{MT}}$  product slightly falls to  $7.256 \text{ cm}^3 \text{ K mol}^{-1}$  at 55 K and then rises to a high value of  $12.26 \text{ cm}^3 \text{ K mol}^{-1}$  at 10 K. This implies the population of a triplet state on lowering the temperature. A sudden fall of the  $\chi_{\text{MT}}$  product to  $4.745 \text{ cm}^3 \text{ K mol}^{-1}$  has been seen below 10 K. This low temperature fall of the  $\chi_{\text{MT}}$  value reveals the depopulation of the triplet state at low thermal energy due to presence of magnetic anisotropy (zero field splitting) in the Co(II) ion. This is also in agreement with the field-cooled-zero-field-cooled protocol (100 Oe) which shows a transition peak at around 10 K (Fig. 6). The best fit is obtained for the above  $\chi_{\text{MT}}$  behavior considering a bilinear exchange term  $2J$  associated with single ion anisotropy (D), by the following spin Hamiltonian (1).

$$\hat{H} = g_1 \mu_B \hat{B} \hat{S}_1 + g_2 \mu_B \hat{B} \hat{S}_2 - 2J_{\text{Co-Co}} \hat{S}_1 \cdot \hat{S}_2 + D_{11} \left[ \hat{S}_{1z}^2 - \frac{1}{3} \hat{S}_1 (\hat{S}_1 + 1) \right] + D_{22} \left[ \hat{S}_{2z}^2 - \frac{1}{3} \hat{S}_2 (\hat{S}_2 + 1) \right] + E_{11} \left( \hat{S}_{1x}^2 - \hat{S}_{1y}^2 \right) + E_{22} \left( \hat{S}_{2x}^2 - \hat{S}_{2y}^2 \right) \dots \dots \dots (1)$$

where the specific terms have their usual meanings.

**Table 3.**

The same values of the Lande  $g$  factors ( $g_1$  and  $g_2$ ) and the ZFS terms ( $D_1$  and  $D_2$ ) are assumed for the two oxo-bridged Co(II) ions ( $S_1$  and  $S_2$ ). The field dependent magnetization data were fitted by fixing the  $g$  values obtained from the  $\chi_{\text{MT}}$  fit ( $(g_{x,y} = 2.91; g_z = 2.18)$ ) (Fig. 7). Both the fits of  $\chi_{\text{MT}}$  and the magnetization data provide ferromagnetic exchange coupling ( $2J = + 10.3 \text{ cm}^{-1}$ ) and high single-ion magnetic anisotropy ( $D = + 29.8 \text{ cm}^{-1}$ ,  $E = + 1.6 \text{ cm}^{-1}$ ) values. Good agreement factors ( $R^2$ ) in the order of  $10^{-4}$  are obtained in all the least squares fitting processes. The high positive zero-field splitting originates from the distortion of the coordination geometry from the ideal square pyramidal geometry. A ferromagnetic exchange interaction is also observed from the experimental magnetization data as it shows saturation in magnetization (4.9

$/N\beta$ ) at high field with a coercivity of 200 Oe (2K), as shown in Fig. S4. The small intermetallic Co(II)•••Co(II) distance (3.198 Å) and the borderline bridge angle (99.3°) favours a suitable overlap for the ferromagnetic exchange coupling in the dimeric moiety. The complex exhibits intermolecular  $\pi$ ••• $\pi$  ordering (offset, 4.086 Å) between the two co-facial pyrazole moieties, which might also mediate the weak ferromagnetic exchange interaction between the two paramagnetic Co(II) ions. In conclusion, the present Co(II) dimeric complex possesses a high positive magnetic anisotropy ( $D = + 29.8 \text{ cm}^{-1}$ ) and a weak ferromagnetic exchange interaction ( $J = + 10.3 \text{ cm}^{-1}$ ). It shows complete magnetic hysteresis curves at several temperatures (Fig. 8). The inset shows the appearance of a coercivity of 200 Oe at 2K, an indication of a soft ferromagnet.

The two reported pentacoordinated Co(II) dimers [ $\{\text{Co}[\text{O}_2\text{NN}']^{\text{AmAmPy}}\}_2$ ] and  $[\text{Co}_2(\text{TPA})_2(\mu\text{-tp})](\text{ClO}_4)_2 \cdot 2\text{H}_2\text{O}$  [38.39] exhibited ferro- and antiferromagnetic coupling with  $2J$  values of  $>0.2$  and  $-0.8 \text{ cm}^{-1}$ , respectively (Table 3). The ZFS  $D$  parameter for the latter is only  $7.3 \text{ cm}^{-1}$ . However, in the present investigation the dimeric neutral Co(II) complex  $[\text{Co}_2(\text{L})_2(\text{N}_3)]$  exhibits comparatively higher  $2J$  and  $D$  values than the so far reported pentacoordinated Co(II) dimers.

**Fig. 6**

**Fig. 7**

**Fig. 8**

### EPR spectra

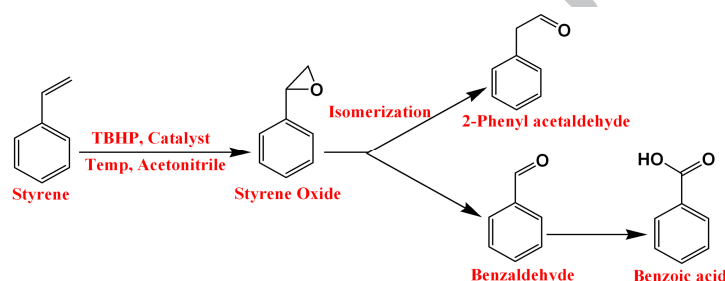
EPR spectroscopy is a powerful technique which is sensitive towards the electronic structure of paramagnetic species. The X-band (9.5 GHz) EPR spectra (Fig. 9) of the sample (solid phase) containing the Co(II) ion in a distorted square-pyramidal geometry was run at 77 K in a liquid nitrogen finger dewar. The experiment shows two derivative signals of  $S = 3/2$  species with resonance at  $g \approx 2.141$  ( $g_z$ ) and 2.951 ( $g_{x,y}$ ). The appearance of a high anisotropic rhombic  $g_{x,y}$  value is evidenced from the low field splitting at 2.951 and the corresponding high field splitting is responsible for the axial splitting ( $g_z$ ). The appearance of a high anisotropic  $g_z$  value is evidenced from the low field splitting at 2.951. From the spectra, it is seen that the experimental Lande splitting factor is in close agreement with the theoretical values obtained from magnetic

fitting procedures.

**Fig. 9**

### Catalytic activity

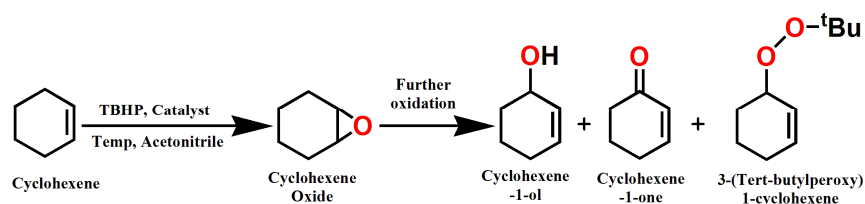
A keen study of the catalytic activity of the neutral cobalt(II) dimer  $[\text{Co}_2(\text{L})_2(\text{N}_3)_2]$  (**1**) towards the oxidation of different common olefins, like styrene, cyclohexene and cyclooctene, under homogeneous conditions has been carried out in a small volume of MeCN using TBHP as the oxygen donor and the corresponding results are presented in Table 4.



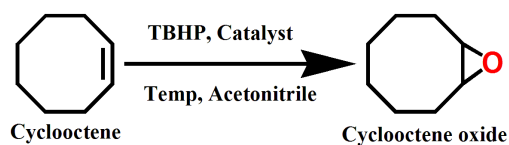
**Scheme 2:** Various oxidation products of styrene using TBHP and the Co complex.

**Table 4.**

The oxidation of styrene using TBHP initially produces styrene oxide, which is converted to the more stable benzaldehyde product, and after prolonged oxidation it produces a small amount of benzoic acid. In another parallel reaction some styrene oxide isomerizes to generate small amount of 2-phenyl acetaldehyde, as outlined in Scheme 2. Our catalyst shows an appreciable conversion of styrene to give a high yield of benzaldehyde



**Scheme 3:** Oxidation products of cyclohexene in the presence of TBHP.



**Scheme 4:** Oxidation of cyclooctene in the presence of TBHP and the Co catalyst.

Similarly, several products are formed from cyclohexene oxidation, which is presented in Scheme 3. Among these products cyclohexene-1-one is the major product obtained, with above 80% selectivity (Entry 2, Table 4). On the other hand, cyclooctene, on oxidation under similar conditions, exhibits a good conversion to offer a reasonable amount of cyclooctene oxide (Scheme 4, Entry 3, Table 4). The time based conversion of all these alkenes and the formation of the various products are graphically shown in (Fig. S5). From Fig. 10 it is observed that although benzaldehyde is the only product (100% selectivity) up to 8 h, the total yield is not so high (ca. 36%). After 24 h the conversion of styrene is increased appreciably, but due to the formation of other by-products, like styrene oxide, benzoic acid etc., the selectivity or % yield of benzaldehyde decreases to 75%. In the case of cyclohexene, initially the main product is formed in a small amount owing to formation of epoxide, alcohol and a TBHP derivative. As the time of reaction is increased the amount of those products goes down, enhancing the selectivity of the ketone (major, about 80%). Without the aid of a catalyst almost no conversion is observed for cyclohexene, despite using the same amount of TBHP (Entry 5, Table 4).

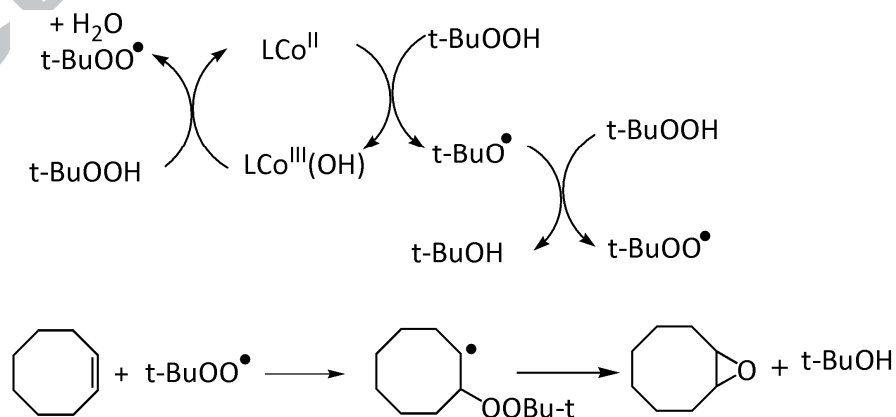
**Fig. 10.**

**Fig. 11**

In order to optimize the effect of the TBHP amount on this oxidation reaction we have also carried out the reaction with a cyclohexene:TBHP molar ratio of 1:1 and it is observed that although the conversion after 24 h is slightly higher than that with a 2:1 ratio, the selectivity towards the main product decreases drastically to ca. 64% (Entry 4) with a subsequent increase in the amounts of the by-products. The amounts of the different products after 24 h conversion with both molar ratios (2:1 and 1:1) is clearly shown in Fig. 11. Thus it can be concluded that 2:1 is the best substrate:oxidant ratio for this catalytic reaction condition. We have also tried to carry

out the same catalytic reaction using  $\text{H}_2\text{O}_2$  as an oxidant, and it was astonishingly observed that there is no catalytic conversion of olefins. A reasonable explanation may be furnished by considering the fact that the intermediate that is formed by the reaction of the complex with  $\text{H}_2\text{O}_2$  is quite stable and stops the catalytic cycle here. We have performed HRMS studies which suggests the formation of  $[\text{Co}_2(\text{L})_2(\text{HO}_2)_2]$  species where the two azide ions are replaced by two hydroperoxide ( $\text{HOO}^-$ ) species (Figure S8).

The catalytic oxidation of olefins may occur either through a radical or concerted pathway [40]. In order to get a clear picture of the mechanistic detail we have carried out the catalytic reactions in the presence of a radical scavenger, like 2,4-di-*tert*-butylphenol. After 24 h it is observed that only 7 and 11% conversions are observed in the case of styrene and cyclooctene, respectively, clearly supporting the operation of a radical pathway over the concerted one. Here, in Scheme 5 (as a representative example for cyclooctene), the first step involves the reductive cleavage of the peroxide bond of *t*-BuOOH by  $\text{LCo}^{\text{II}}$  to form *t*-BuO $\cdot$  and  $\text{LCo}^{\text{III}}(\text{OH})$ . The *t*-BuO $\cdot$  radical in turn rapidly abstracts a hydrogen atom from *t*-BuOOH to form the thermodynamically more stable *t*-BuOO $\cdot$  [41]. Now the one electron oxidation of *t*-BuOOH by  $\text{LCo}^{\text{III}}(\text{OH})$  leads to the formation of *t*-BuOO $\cdot$  and  $\text{H}_2\text{O}$ , and regenerates  $\text{LCo}^{\text{II}}$ , thereby completing one catalytic cycle. Thus, in one complete catalytic cycle three mole of *t*-BuOOH are used up to generate one mole of *t*-BuOH, one mole of water and two moles *t*-BuOO $\cdot$ . The *t*-BuOO $\cdot$  radical thereby generated now reacts with cyclooctene to generate cyclooctene-oxide. The same mechanism was found to be operative for the other olefins.



Scheme 5

## Conclusions

The present study demonstrates an interesting coordination compound obtained from a tridentate ligand, 2,6-bis-(3,5-dimethyl-pyrazol-1-ylmethyl)-4-methyl-phenol (HL), where two ligands are coordinated to two cobalt atoms. X-ray crystallographic studies revealed that in the complex both the cobalt atoms are in the +2 oxidation state, as supported by BVS calculations. Low temperature magnetic studies showed that the present Co(II) dimeric complex, devoid of any single molecule magnetic behavior, possesses high positive magnetic anisotropy ( $D = +29.8 \text{ cm}^{-1}$ ) and a weak ferromagnetic exchange interaction ( $J = +10.3 \text{ cm}^{-1}$ ). It shows the complete magnetic hysteresis curves at several temperatures, with the appearance of coercivity of 200 Oe at 2K, an indication of a soft ferromagnet. The catalytic epoxidation of cyclohexene, styrene and cyclooctene by *t*-BuOOH has been explored in MeCN, which appeared to proceed through a radical pathway with modest TONs and quite an impressive selectivity towards epoxides.

## References

- [1] S. J. Lippard and M. Berg, Principles of Bioinorganic Chemistry; University Science Books: Mill Valley, CA, (1994); Chapter 12.
- [2] (a) J. Halpern, Science 227 (1985) 869; (b) M. K. Geno, J. Halpern, J. Am. Chem. Soc. 109 (1987) 1238.
- [3] M. F. Perutz, G. Fermi, B. Luisi, B. Shaanan, R. C. Liddington, Acc. Chem. Res. 20 (1987) 309.
- [4] A. L. Raphael, H. B. Gray, J. Am. Chem. Soc. 113 (1991) 1038.
- [5] T. P. J. Garret, D. J. Glingeleffer, J. M. Guss, S. J. Rogers, H. C. Freeman, J. Biol. Chem. 259 (1984) 2822.
- [6] B. E. Schultz, S. F. Gheller, M. C. Muetterties, M. J. Scott, R. H. Holm, Acc. Chem. Res. 19 (1986) 363.
- [7] D. Sellmann, J. Sutter, Acc. Chem. Res. 30 (1997) 460.
- [8] S. L. Roderick, B. W. Matthews, Biochemistry 32 (1993) 3907.
- [9] R. E. P. Winpenny, J. Chem. Soc., Dalton Trans. (2002) 1.
- [10] J. Narayanan, A. S.-Peralta, V.M. U.-Saldivar, R. Escudero, H. Höpfl, M.E.S.-Torres, Inorg. Chim. Acta 361 (2008) 2747.
- [11] D. Gatteschi, R. Sessoli, Angew. Chem., Int. Ed. 42 (2003) 268.

- [12] S. K. Ritter, Chem. Eng. News 82 (2004) 29.
- [13] R. Sessoli, H.-L. Tsai, A.R. Schake, S. Wang, J.B. Vincent, K. Folting, D. Gatteschi, G. Christou, D.N. Hendrickson, J. Am. Chem. Soc. 115 (1993) 1804.
- [14] W. Wernsdorfer, Adv. Chem. Phys. 118 (2001) 99.
- [15] J. Liang, Q. Zhang, H. Wu, G. Meng, Q. Tang, Y. Wang, Catal. Commun. (2004) 5.
- [16] T. Mukaiyama, K. Yorozu, Y. Takai, T. Yamada, Chem. Lett. (1993) 439.
- [17] R. A. Budnik, J. K. Kochi, J. Org. Chem. 41 (1976) 1384.
- [18] D.E. Hamilton, R.S. Drago, A. Zombeck, J. Am. Chem. Soc. 109 (1987) 374.
- [19] B. Rhodes, S. Rowling, P. Tidswell, S. Woodward, S.M. Brown, J. Mol. Catal. A: Chem. 116 (1997) 375.
- [20] R. I. Kureshy, N. H. Khan, S. H. R. Abdi, A.K. Bhatt, P. Iyer, J. Mol. Catal. A 121 (1997) 25.
- [21] P. Buranaprasertsuk, Y. Tangsakol, W. Chavasiri, Catal. Commun. 8 (2007) 310.
- [22] A. Zhang, L. Li, J. Li, Y. Zhang, S. Gao, Catal. Commun. 12 (2011) 1183.
- [23] M.J. da Silva, P. Robles-Dutenhefner, L. Menini, E.V. Gusevskaya, J. Mol. Catal. A: Chem. 201 (2003) 71.
- [24] M.J. Beier, W. Kleist, M.T. Wharmby, R. Kissner, B. Kimmerle, P.A. Wright, J.-D. Grunwaldt, A. Baiker, Chem. Eur. J. 18 (2012) 887.
- [25] X. -Y. Quek, Q. Tang, S. Hu, Y. Yang, Appl. Catal. A 361 (2009) 130.
- [26] Z. Opere, T. Mallat, A. Baiker, J. Catal. 245 (2007) 482.
- [27] S. Biswas, A. Dutta, M. Debnath, M. Dolai, K.K. Das, M. Ali, Dalton Trans. 42 (2013) 13210.
- [28] G.M. Sheldrick, SAINT (Version 6.02), SADABS (Version 2.03), Bruker AXS Inc., Madison, Wisconsin, 2002.
- [29] (a) G.M. Sheldrick, Acta Crystallogr., Sect. A: Found. Crystallogr. 64 (2007) 112; (b) G.M. Sheldrick, SHELXL-97, Crystal Structure Refinement Program, University of Göttingen 1997.
- [30] (a) G.J. Palenik, Inorg. Chem. 36 (1997) 122; (b) M. Dolai, A. Amjad, M. Debnath, J. van Tol, E.del Barco, M. Ali, Inorg. Chem. 53 (2014) 5423.
- [31] A. D. Kent, S. von Molnár, S. Gider, D.D. Swschalom, J. Appl. Phys. 76 (1994) 6656.



- [32] D.A. Safin, P. Mlynarz, F.E. Hahn, M.G. Babashkina, F.D. Sokolov, N.G. Zabirov, J. Galezowska, H. Kozlowski, Z. Anorg. Allg. Chem. 633 (2007) 1472.
- [32] R. Herchel, R. Boca, Dalton Trans. (2005) 1352.
- [32] F.H. Zhao, Y.-X. Che, J.-M. Zheng, F. Grandjean, G.J. Long, Inorg. Chem. 51 (2012) 4862.
- [35] J.M. Zadrozny, J. Liu, N.A. Piro, C.J. Chang, S. Hill, J.R. Long, Chem. Commun. 48 (2012) 3897.
- [36] J.M. Zadrozny, J.R. Long, J. Am. Chem. Soc. 133 (2011) 20732.
- [37] D. Nelson, L.W. ter Haar, Inorg. Chem. 32 (1993) 182.
- [38] U.K. Das, J. Bobak, C. Fowler, S.E. Hann, C.F. Petten, L.N. Dawe, A. Decken, F.M. Kerton, C.M. Kozak, Dalton Trans. 39(2010) 5462.
- [39] S.S. Massoud, K.T. Broussard, F.A. Mautner, R. Vicente, M.K. Sah, I. Bernal, Inorg. Chim. Acta 361 (2008) 123.
- [40] (a) J. Zhang, A.V. Biradar, S. Pramanik, T.J. Emge, T. Asefa, J. Li, Chem. Commun. 48 (2012) 6541; (b) M. Yonemitsu, Y. Tanaka, M. Iwamoto, J. Catal. 178 (1998) 207; (c) R. D. Oldroyd, J. M. Thomas, T. Maschmeyer, P. A. MacFaul, D. W. Snelgrove, K. U. Ingold, D.D.M. Wayner, Angew. Chem., Int. Ed. Engl. 35 (1996) 2787; (d) J. Sebastian, K.M. Jinka, R.V. Jasra, J. Catal. 244 (2006) 208; (e) J. Hudak, R. Boca, J. Moncol, J. Titis, Inorg. Chim. Acta 394 (2013) 401; (f) J. Hudak, R. Boca, L. Dlhan, J. Kozisek, J. Moncol, Polyhedron 30 (2011) 1367; (g) R. Herchel, R. Boca, Dalton Trans. (2005) 1352; (h) C. Rajnak, J. Titis, O. Fuhr, M. Ruben, R. Boca, Inorg. Chem. 53 (2014) 8200; (i) C. Rajnak, J. Titis, I. Salitros, R. Boca, O. Fuhr, M. Ruben, Polyhedron 65 (2013) 122.
- [41] (a) D.W. Snelgrove, J. Lusztyk, J.T. Banks, P. Mulder, K.U. Ingold, J. Am. Chem. Soc. 123 (2001) 469; (b) P.A. MacFaul, I.W.C.E. Arends, K.U. Ingold, D.D.M. Wayner, J. Chem. Soc., Perkin Trans 2, 2 (1997) 135.

**Table 1.** Crystallographic and structure refinement data for complex **1**.

Formula	$C_{38}H_{46}Co_2N_{14}O_2$ (CCDC 1062604)
Formula Weight	848.75
Crystal System	Monoclinic
Space group	C2/c (No. 15)
a [Å]	20.0837(6)
b [Å]	11.6348(3)
c [Å]	17.1398(6)
$\alpha$ [°]	90
$\beta$ [°]	108.024(4)
$\gamma$ [°]	90
V [Å <sup>3</sup> ]	3808.5(2)
Z	4
D(calc) [g/cm <sup>3</sup> ]	1.480
Mu(MoK $\alpha$ ) [mm <sup>-1</sup> ]	0.927
F(000)	1768
Temperature [K]	150
Radiation [Å] MoK $\alpha$	0.71073
$\theta$ Min-Max [°]	3.0, 25.1
Dataset	-23: 23; -13: 13; -20: 20
Tot., Uniq. Data, R(int)	17358, 3391, 0.035
Observed data [I > 2.0 sigma(I)]	2814
N <sub>ref</sub> , N <sub>par</sub>	3391, 266
R, wR <sub>2</sub> , S	0.0310, 0.0762, 1.02

**Table 2.** Selected bond distance and bond angles of **1**

Bond distance (Å)			
Co1–O1	2.1929(15)	O1–Co1–O1a	80.47(5)
Co1–N1	2.0495(18)	N1–Co1–N3	92.41(7)
Co1–N3	2.1563(19)	N1–Co1–N5	125.31(7)
Co1–N5	2.0165(19)	O1a –Co1–N1	108.15(6)
Co1–O1a	1.9792(14)	N3–Co1–N5	90.65(8)
Bond Angles (°)		O1a –Co1–N3	100.90(6)
O1–Co1–N1	86.21(6)	O1a –Co1–N5	124.73(7)

Symmetry a = 1-x, y, 1/2-z

**Table 3.** Magnetic data of some relevant dinuclear cobalt(II) complexes.

Complex	$2J$ (cm <sup>-1</sup> )	$D$ (cm <sup>-1</sup> )	Ref.
$[\{Co(O_2NN^{\gamma}AmAmPy)\}_2]^a$	<0.2	-----	[38]
$[Co_2(TPA)_2(\mu-tp)](ClO_4)_2 \cdot 2H_2O^a$	-0.8	7.3	[39]
$[Co_2(L)_2(N_3)_2]^a$	10.3 <sup>b</sup>	+ 29.8 <sup>b</sup>	This work
$[Co_2(H_2O)(PhCO_2)_4(py)_4] \cdot 0.5(PhCO_2H) \cdot 1.5(MePh)$	-1.90	+92.4	[40(e)] <sup>c</sup>
$[Co_2(H_2O)(PhCO_2)_4(Mepy)_4]$	-0.70	+50.7	
$[Co_2(H_2O)(PhCO_2)_4(iqu)_4] \cdot iqu$	-2.43	+99.6	
$[Co_2(H_2O)(PhCO_2)_4(fupy)_4]$	-0.90	+68.7	
$[Co_2(H_2O)(PhCO_2)_4(Mefupy)_4]$	-1.63	+79.9	
$[Co_2(H_2O)(PhCO_2)_4(Me_2fupy)_4]$	-1.12	+77.5	
$trans-[Co(bz)_2(H_2O)_2(nca)_2]$	None	+94.1	[40(f)] <sup>c</sup>
$[Co_2(\mu-PhCOO)_4(qu)_2]$	-1.65	+67.2	
$[Co_3(\mu-bz)_4(bz)_2(inca)_6]$	-1.51	+54.7	
$CoL^5$	-----	+48.4	[40(g)] <sup>a</sup>
$[CoL_3Cl_2]$	+1.4	+151	[40(h)] <sup>a</sup>
$CoCl_2L^1$	-0.075	+ 71.7	[40(i)]
$[CoCl_2L^2]$	- 0.026	+ 46.8	

<sup>a</sup> pentacoordinated cobalt(II); <sup>b</sup> 0.1 T; <sup>c</sup> hexacoordinated

**Table 4.** Oxidation of olefins (0.25 g) over the Co-pyrazole complex (1).

Entry	Substrate	Conversion (%)	Main product	Selectivity (%)
1	Styrene	58.50	Benzaldehyde	75.47
2	Cyclohexene	94.18	cyclohexene-1-one	80.45
3	Cyclooctene	78.13	cyclooctene-oxide	66.81

<b>4</b>	Cyclohexene <sup>a</sup>	98.86	cyclohexene-1-one	63.93
<b>5</b>	Cyclohexene <sup>b</sup>	0.33	-	-

Reaction conditions: substrate:TBHP = 2:1 molar ratio, MeCN = 2 ml, catalyst = 0.05 g, temperature = 50-55 °C, time = maximum 24 h. <sup>a</sup>reaction carried out with substrate:TBHP = 1:1 molar ratio, <sup>b</sup>reaction was performed without catalyst.

### Figure Captions

- Fig. 1** Molecular view with the atom numbering of **1**, symmetry  $a = 1-x, y, 1/2-z$ . All H-atoms are omitted for clarity.
- Fig. 2**  $\pi \cdots \pi$  bonding as well as H-bonding interactions of complex **1** resulting in a 1D chain.
- Fig. 3** Packing diagram of complex **1** showing the hydrogen bonded 3D-layers.
- Fig. 4** UV-Vis spectra of L and complex **1** in CH<sub>3</sub>CN with  $[c] = 1.0 \times 10^{-3}$  M.
- Fig. 5** CV of complex **1** in MeCN solvent at 25°C,  $[c] = 1.0$  mM; [TBAPC] = 0.10 M, scan rate = 100 mVs<sup>-1</sup>
- Fig. 6** The temperature dependence of the magnetic susceptibility measured at 100 Oe using a field-cooled-zero-field-cooled protocol. Inset reveals the splitting of the ZFC and FC curves at low temperature.
- Fig. 7** The variation of  $\chi_M T$  with temperature for the Co(II) dimeric complex. Solid line represents the theoretical curve and the points show the experimental data.
- Fig. 8** The complete magnetic hysteresis curves at several temperatures. Inset shows the appearance of coercivity of 200 Oe at 2K, an indication of a soft ferromagnet.
- Fig. 9** EPR spectrum of the  $S = 3/2$  Co(II) system showing a high anisotropy axial signal at  $g \approx 2.951$  for solid phase.
- Fig. 10** Time dependent conversion of styrene and formation of benzaldehyde.
- Fig. 11** Effect of substrate:TBHP ratio on the yield of different products of cyclohexene.

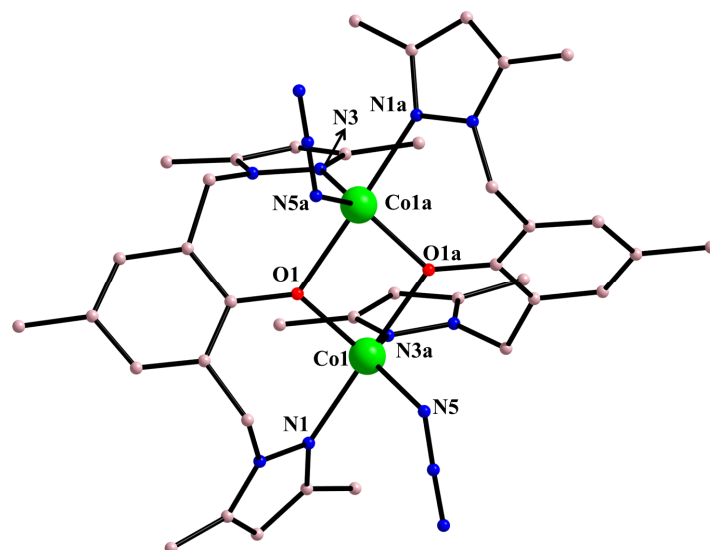


Fig. 1

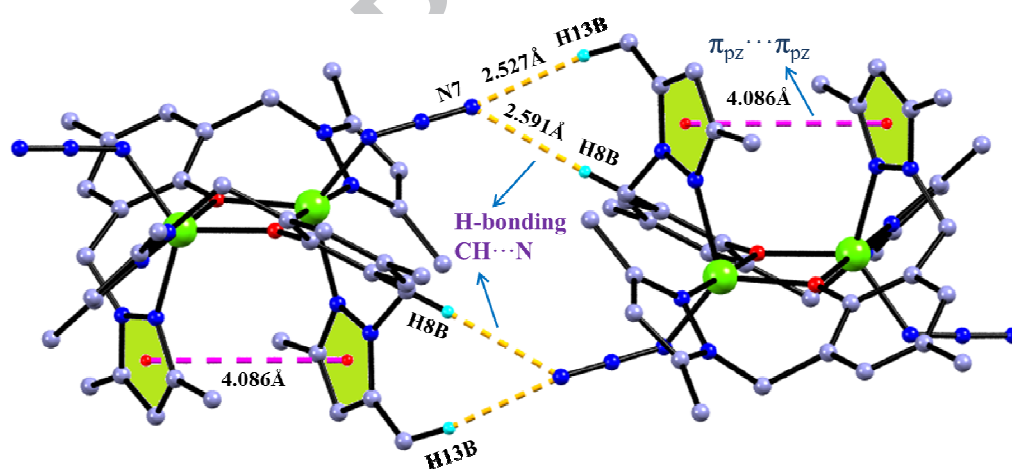


Fig. 2

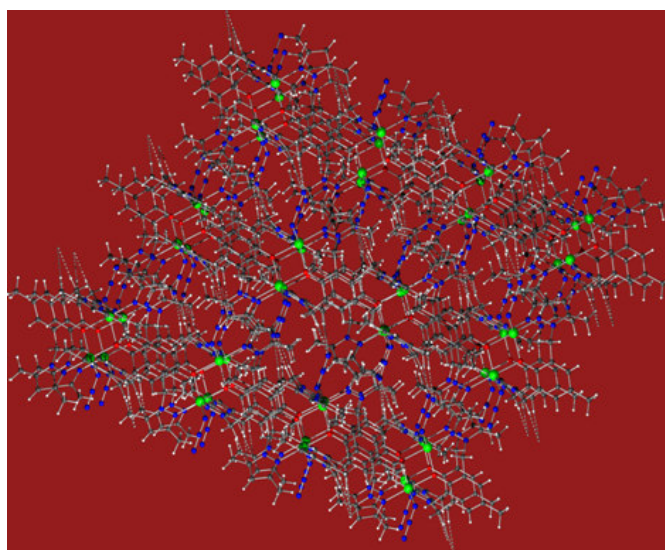


Fig. 3

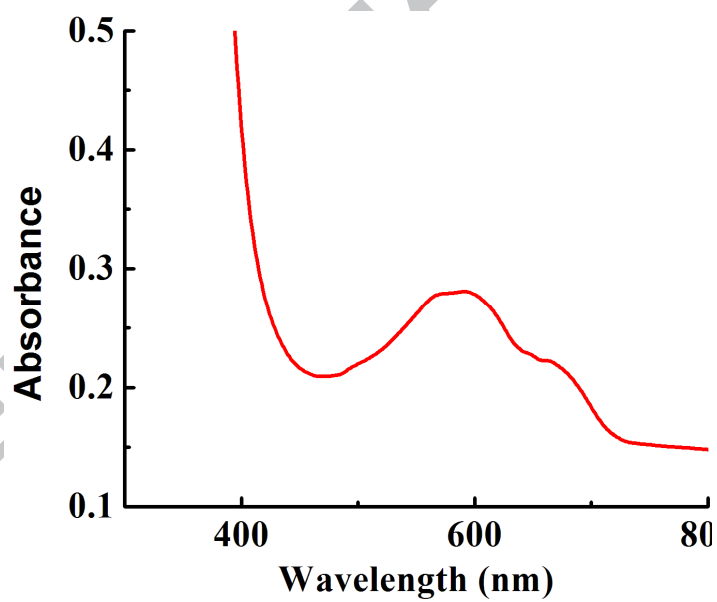


Fig. 4

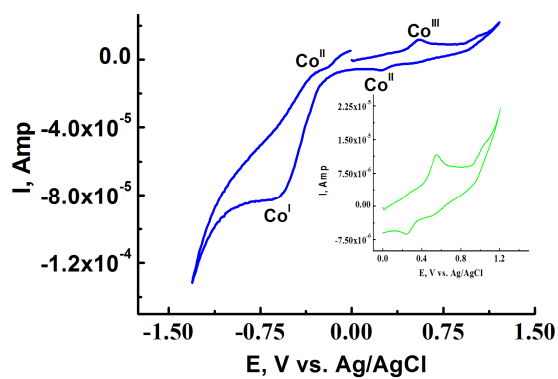


Fig. 5

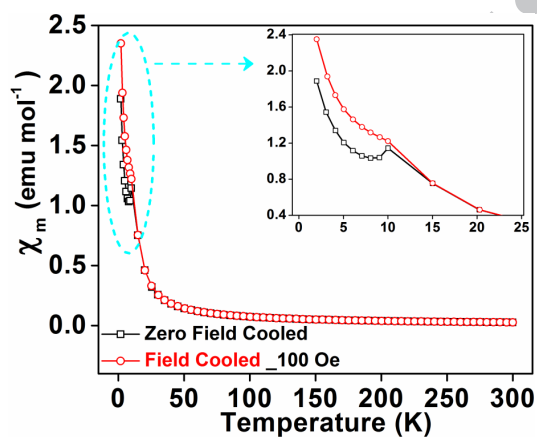


Fig. 6

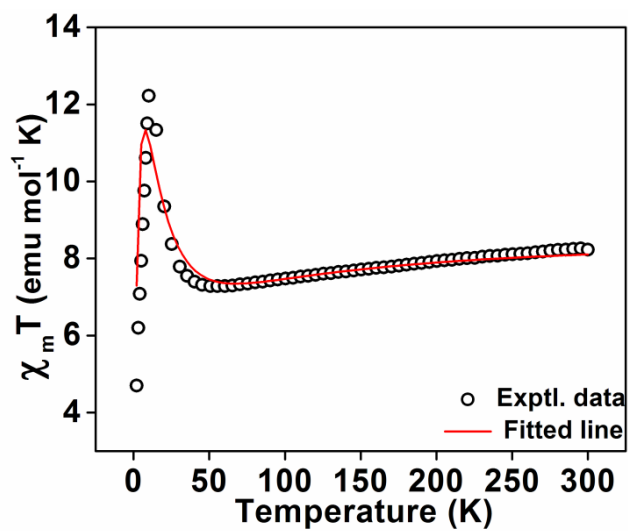


Fig. 7



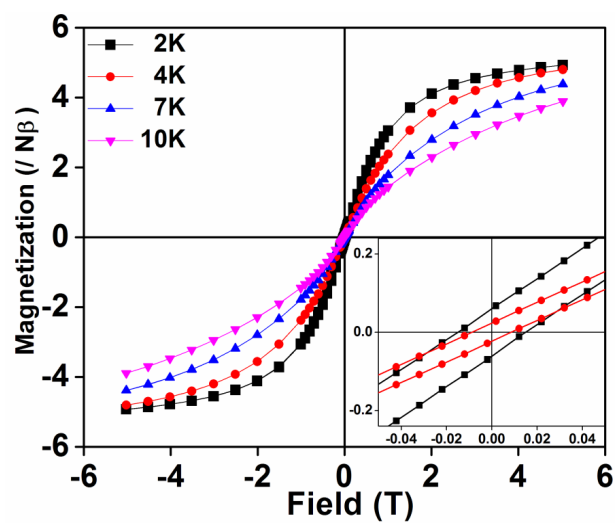


Fig. 8

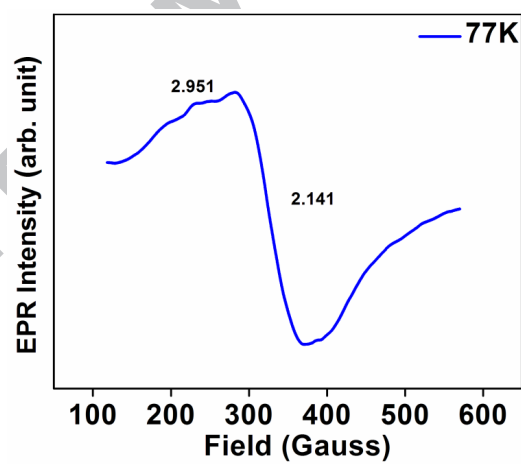


Fig. 9

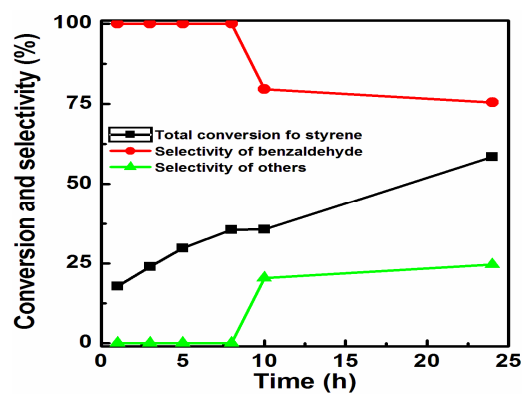


Fig. 10

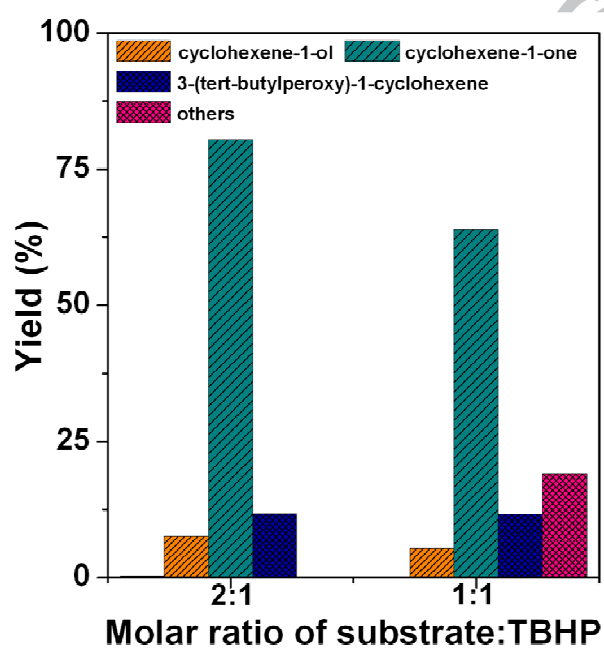
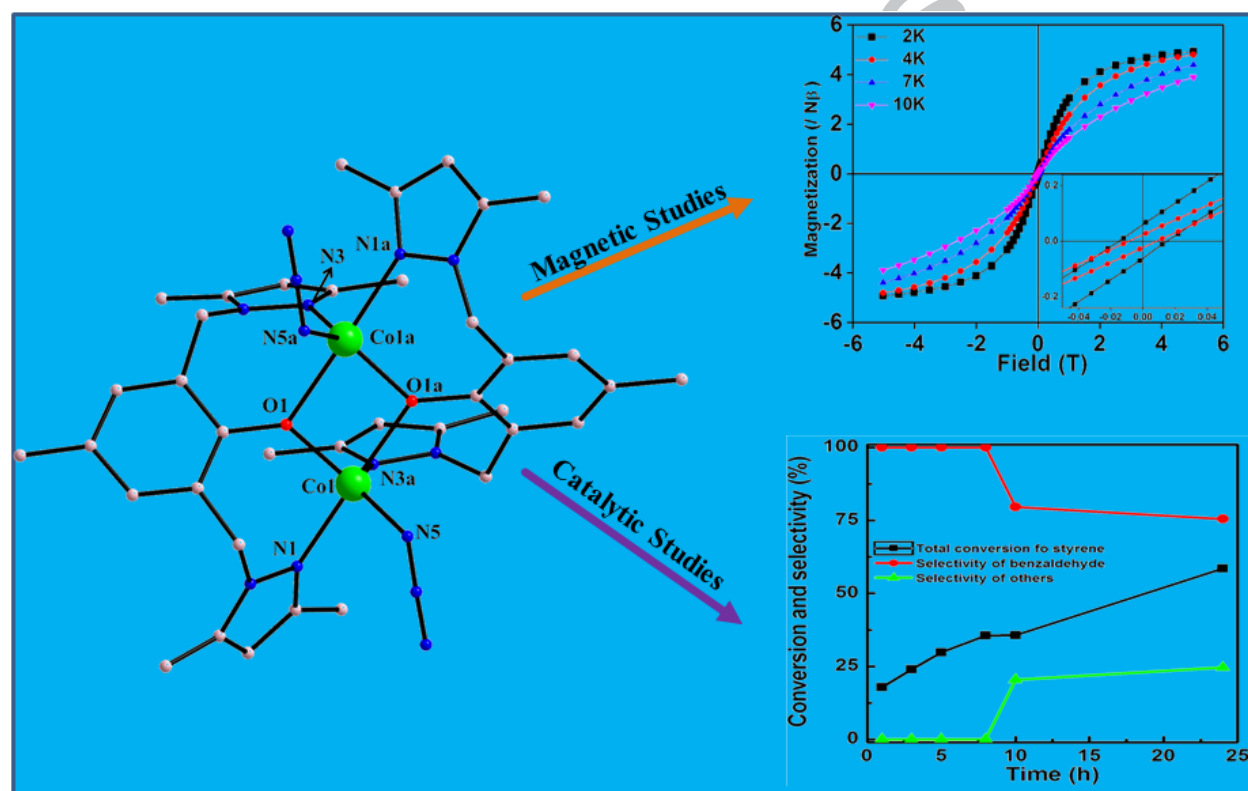


Fig. 11

## Synthesis, structure, catalytic and magnetic properties of a pyrazole based five coordinated di-nuclear cobalt(II) complex

Rabiul Alama, Kaberi Pala, Bikash Kumar Shawb, Malay Dolaia, Nabanita Pala, Shyamal Kumar Sahab and Mahammad Alia\*

A five coordinated dinuclear cobalt(II) complex,  $[\text{Co}_2(\text{L})_2(\text{N}_3)_2]$  (**1**), displayed modest catalytic activity towards the oxidation of various allylic compounds. Low temperature magnetic studies gives high positive magnetic anisotropy ( $D = +29.8 \text{ cm}^{-1}$ ) and a weak ferromagnetic exchange interaction ( $J = +10.3 \text{ cm}^{-1}$ ).



## Synthesis, structure, catalytic and magnetic properties of a pyrazole based five coordinated di-nuclear cobalt(II) complex

Rabiul Alama, Kaberi Pala, Bikash Kumar Shawb, Malay Dolaia, Nabanita Pala, Shyamal Kumar Sahab and Mahammad Alia\*

A five coordinated dinuclear cobalt(II) complex,  $[\text{Co}_2(\text{L})_2(\text{N}_3)_2]$  (**1**), displayed modest catalytic activity towards the oxidation of various allylic compounds. Low temperature magnetic studies gives high positive magnetic anisotropy ( $D = +29.8 \text{ cm}^{-1}$ ) and a weak ferromagnetic exchange interaction ( $J = +10.3 \text{ cm}^{-1}$ ).